Polym. Bull. (2011) 67:1261–1271
DOI 10.1007/s00289-011-0485-0

ORIGINAL PAPER

Preparation and characterization of PLLA–ESO/surface-grafted silica nanocomposites

Jun Zou · Teng Ma · Jing Zhang · Wei He · Farong Huang

Received: 24 October 2010 / Revised: 2 April 2011 / Accepted: 11 April 2011 /
Published online: 20 April 2011

Abstract Various amounts of surface-grafted silica (g-SiO_2) and un-grafted (SiO_2) nanoparticles were solution blended with a copolymer of L-lactide and epoxidized soybean oil (PLLA–ESO) or PLLA. Chemical reaction between the low molecular weight (LMW) PLLA and surface of silica nanoparticles is confirmed by FTIR and TGA analyses. The amount of grafted LMW PLLA investigated by thermal gravimetric analysis (TGA) was about 14.9%–28.2% in weight. g-SiO_2 nanoparticles can be easily dispersed into PLLA–ESO matrix to form a uniform PLLA–ESO/g-SiO_2 composite. Thermal properties of PLLA–ESO/g-SiO_2 and PLLA/g-SiO_2 nanocomposites were subsequently investigated by the differential scanning calorimeter measurements (DSC). DSC analyses indicated that g-SiO_2 nanoparticles can serve as a nucleating agent for the crystallization of PLLA–ESO in the composites, while the melting temperature (T_m) and the glass transition temperature (T_g) of PLLA–ESO/g-SiO_2 nanocomposites seemed to be independent of loading of g-SiO_2 particles. The DSC curves of PLLA/g-SiO_2 nanocomposite obviously showed double melting peaks, while that of PLLA–ESO/g-SiO_2 nanocomposites only a single melting peak. PLLA–ESO/g-SiO_2 composites exhibited a higher tensile strength and elongation than that of PLLA–ESO/SiO_2 composites.

J. Zou (✉) · T. Ma · J. Zhang · W. He
School of Materials Science and Engineering, Jiangsu University of Science and Technology, Zhenjiang 212003, Jiangsu, People's Republic of China
e-mail: zj_881996@163.com

J. Zou · F. Huang
Key Laboratory for Specially Functional Polymeric Materials and Related Technology of the Ministry of Education, School of Materials Science and Engineering, East China University of Science and Technology, Shanghai 200237, People's Republic of China

Keywords Nanocomposites · Surface-grafted silica · Star-shaped copolymer

Introduction

Poly(L-lactide)s (PLLA) were regarded as one of the most promising biodegradable polymers and was expected to substitute some of the non-biodegradable plastics [1, 2]. However, it has inherent low toughness and low crystallization rate [2, 3] which restrict the range of applications. PLLA has been blended with immiscible or miscible polymers [3–6] to enhance its physical properties, thus widening its applicability. However, most of the polymer blends are immiscible, and the multiphase blends show poor mechanical performance because of the low interfacial adhesion between the polymer phases. The promising approaches to overcome these problems are the introduction of units to control the biodegradability and branched structure to improve elasticity, ductility, and/or stabilize the melt viscosity in PLLA. Thus, star-shaped PLLA–ESO copolymers had been synthesized by us [7]. But the crystallinity of the copolymers is still low. Incorporation of silica nanoparticles into PLA has been shown to improve its thermal stability, melt behavior, and mechanical properties [8, 9]. In order to improve interfacial interaction between the surface of silica nanoparticles and the PLA matrix, the nanoparticles of SiO_2 usually have to been modified before use [9, 10]. Thus, if the modified silica nanoparticles are introduced into PLLA–ESO copolymers matrix, the above-mentioned shortcomings are expected to be improved. In addition, the crystallinity of the copolymers should be improved.

In this report, the LMW PLLA were directly grafted onto the surface of silica nanoparticles with silanol groups (Si-OH) by ring-opening polymerization of LLA using $SnOct_2$ as catalyst. The surface-grafting reaction and the properties of the LMW PLLA–grafted SiO_2 (g-SiO_2)/PLLA–ESO nanocomposites were characterized by FTIR, TGA, DSC, and mechanical measurements.

Experimental

Materials

L-lactide was synthesized according to the literature [11], and purified by recrystallization using dry toluene and ethyl acetate as solvent. Epoxidized soybean oil (ESO, epoxide content = 6.9 wt%) was procured from Shindongbang Co, Korea. Prior to copolymerization, both the L-LA and ESO were dried overnight at 50 °C in vacuum. Stannous octoate ($SnOct_2$) was obtained from Sigma and other agents were all of analytical grade and used as received without further purification. Tetraethoxy silane (TEOS) was purchased from SCRC AR, China. PLLA (M_w = 120,000) and LMW PLLA (M_w = 8,000) was prepared in our laboratory.

The star-shaped copolymers of L-lactide and epoxidized soybean oil were synthesized according to the literature [7]. The M_w of the PLLA–ESO (700/4) is about 120,000.

Synthesis of PLLA–ESO(700/4) copolymer

Certain amounts of L-LA, ESO, and $SnOct_2$ were added under nitrogen to a 100 mL flame dried, round-bottomed flask containing a magnetic stir bar. The flask was purged three times with dry nitrogen and sealed with a ground glass stopper. Under magnetic stirring, the flask was immersed in an oil bath at 160 °C for 5 h. The obtained raw product was purified by dissolution in dichloromethane and re-precipitation by methanol, followed by vacuum drying at 60 °C until it reached a constant weight.

Synthesis of silica nanoparticles

Silica nanoparticles were synthesized via modified Stöber process which involves hydrolysis and polycondensation of tetraethylorthosilicate (TEOS) under alkaline conditions in ethanol [12]. The optimal experimental conditions and procedure for the synthesis was referred to the literature [13]. 8 ml ammonia as base catalyst (NH_3 25%, SCRC) containing 4 ml distilled water were mixed with 200 ml Absolute ethanol (AR, SCRC) in a 250 ml conical flask. The flask was first stirred for 1 h. Then, 12 ml TEOS was titrated into the conical flask. The mixture was stirred at 55 °C for 12 h. The sol–gel form was first stirred in EtOH (20 wt% EtOH) to disperse the nanoparticles. Then, the nanoparticles were separated from the solution phase using centrifuge machine (Kubota Corporation, model 5920) operated at 5,000 rpm/10 min. The cycle was repeated for three times and the final product was dried in conventional drying oven at 80 °C for 24 h.

Grafting of LMW PLLA onto the surface of silica nanoparticles

LMW PLLA was grafted onto the surface of silica nanoparticles by ring-opening polymerization of L-lactide using $SnOct_2$ as catalyst. The details of silica surface grafting are briefly described as follows: in a 250 ml conical flask, 25 g L-lactide was dissolved in 100 ml toluene, thereafter, 10 g silica nanoparticles was added into this solution. Then, the mixture was slowly heated to 140 °C under nitrogen with stirring. The reaction was maintained at this temperature for 0–48 h. Then, the reaction mixture was cooled down to a room temperature. LMW PLLA-grafted silica nanoparticles (g-SiO_2) were separated by centrifugation at 20,000 rpm and washed with excessive amount of dichloromethane five times to completely remove the free LMW PLLA. Finally, the separated precipitate was dried in a vacuum oven at 50–60 °C for 24 h to remove the residual dichloromethane.

Preparation of PLLA–ESO/g-SiO_2 and PLLA–ESO/SiO_2 nanocomposites

The nanocomposites of g-SiO_2/PLLA–ESO or SiO_2/PLLA–ESO with various amounts (5, 10, 15, 20, and 30 wt%) of g-SiO_2 or SiO_2 were prepared as follows: pre-weighted and dried g-SiO_2 or SiO_2 nanoparticles were uniformly suspended in dichloromethane via ultrasonic vibration for 30 min, and then the suspensions were added into PLLA/dichloromethane solution, respectively with magnetic stirring.

The mixture was precipitated in a certain amount of anhydrous methanol, and the composites were dried in a vacuum oven at 50 °C for 24 h to remove the residual solvent. Nanocomposite sheets were obtained by compression molding at 20 MPa and 180 °C and then cooled to room temperature under pressure.

Characterization

FTIR spectroscopic analyses were performed on a Perkin-Elmer 2000 spectrometer with KBr discs. The thermal stability of the samples (about 7 mg) was investigated with a TGA (TA-Q600) under nitrogen from room temperature (about 20 °C) to 700 °C at a heating rate of 10 °C/min. TEM (Philips Tecnai 12) was applied to examine the dispersion behavior of silica nanoparticles in PLLA–ESO copolymer matrix. Differential scanning calorimetric analysis (DSC) was carried out on a Perkin-Elmer DSC7 series thermal analysis system with indium standards. Samples of the copolymers (10 mg) were heated to 200 °C at a rate of 10 °C/min. The samples were then quenched to room temperature and subjected to a second run at the rate of 10 °C/min. Tensile properties were measured using a universal testing machine (Instron-5566) at 25 °C at a crosshead speed of 20 mm/min according to ASTMD638.

Results and discussion

Grafting of LMW PLLA on the surface of SiO_2

During the ring-opening polymerization process, LMW PLLA was grafted onto the surface of SiO_2 particles under the catalysis of stannous octanoate ($SnOct_2$). The chemical reaction between the LMW PLLA and SiO_2 particles took place in the mixing. The condensation between the silanol group and LMW PLLA occurred on the nanoparticle surfaces resulted in grafting of LMW PLLA onto the nanoparticles.

Figure 1 shows the FTIR spectra of SiO_2 nanoparticles before and after grafting in different reaction times. The SiO_2 nanoparticles (0 h) are chosen to be analyzed by FTIR spectra. It could be seen that the characteristic peaks at 1105, 804, and 467 cm^{-1}, which can be ascribed to the stretching and bending vibrations of Si–O–Si bonds [14]. After surface grafting of SiO_2 nanoparticles, a new absorption band appears at 1,757 cm^{-1}. The new peak could be attributed to the carbonyl group(C=O) of LMW PLLA on the surface of SiO_2 nanoparticles [15], confirming the grafting carboxyl group of LMW PLLA onto the surface of SiO_2 nanoparticles. The g-SiO_2 nanoparticles obtained for 36 h.

The thermogravimetric analysis (TGA) further provided quantitative evidence of grafting. Figure 2 shows four typical TGA curves. The pure SiO_2 is thermally stable at temperature higher than 700 °C and weight loss is only about 1% which could be attributed to the dehydration of Si-OH and the water adsorbed on the surface of SiO_2 nanoparticles. As shown in Fig. 2, the difference $\left(W_{\text{g-LMW PLLA}}^{\text{g-SiO}_2}\right)$ between the residual weight of g-SiO_2 (6–36 h) and that of SiO_2 (0 h) represents the content of

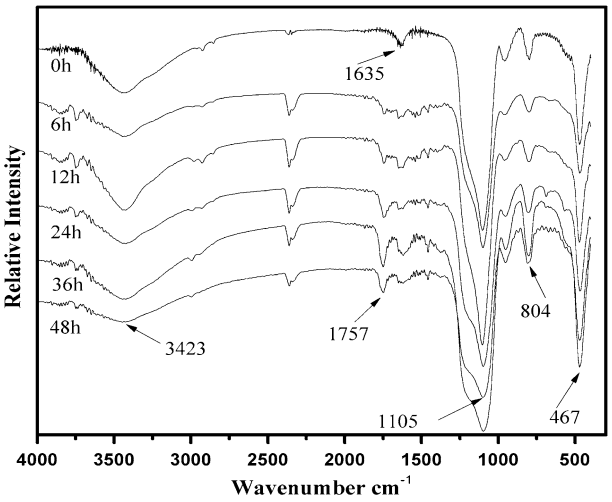

Fig. 1 FTIR spectra of surface modified silica particles obtained in different reaction times exhibit the stronger absorption, thus indicating a maximum grafting ratio of LMW PLLA at this time

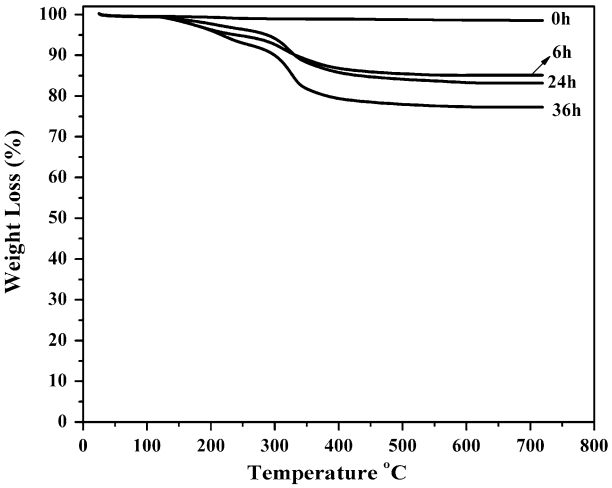

Fig. 2 TGA curves of surface grafting SiO_2 with different reaction times

LMW PLLA in g-SiO_2, while $\left(1 - W_{\text{g-LMW PLLA}}^{\text{g-SiO}_2}\right)$ stands for the net weight of SiO_2 nanoparticles. Therefore, the grafting ratio (G_r) is defined by Eq. 1. As a result, the G_r lies in the range of 14.9–28.2%. The influence of reaction time on the G_r was examined during the reaction time of 6–48 h. This grafting ratio depends on the reaction time as shown in Fig. 3. At 36 h, there appears a maximum grafting ratio of about 28.2%. As confirmed by the absorption intensities of the IR peaks at 2980, 2930, and 1757 cm^{-1} (Fig. 1) of the grafting products, there appeared a maximum of the G_r around 36 h. After that, grafting ratio of LMW PLLA decreased, probably

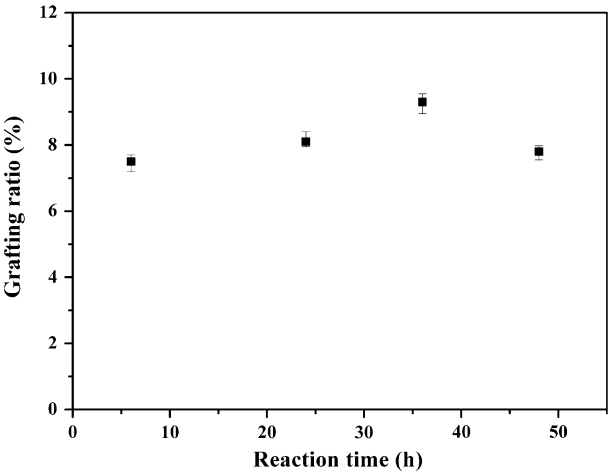

Fig. 3 Grafting ratio determined by TGA as a function of reaction time

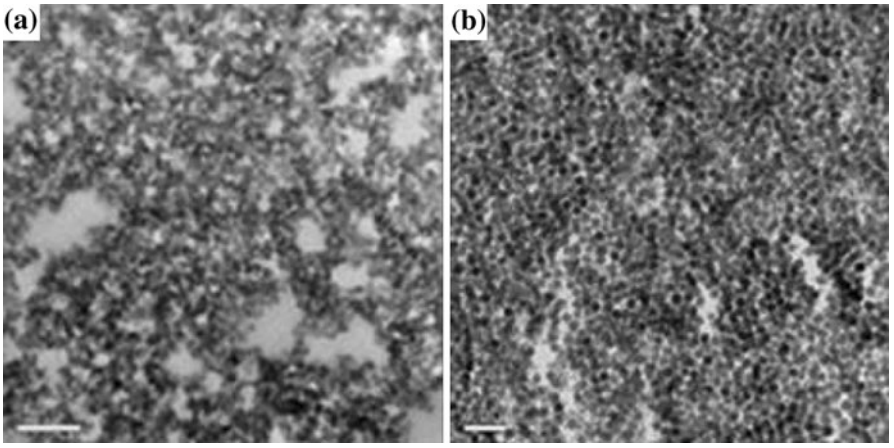

Fig. 4 TEM images of **a** un-grafted SiO_2 and **b** surface grafting SiO_2 nanoparticles dispersed in PLLA–ESO matrix (*scale bar* 500 nm)

due to degradation or transesterification of the PLLA formed [16]. The TGA results also indicate that the non-grafted SiO_2 nanoparticles displays little weight-loss while the grafted ones show appreciable weight-loss. It is ascribed to the decomposition of the grafted LMW PLLA on the surface of SiO_2 nanoparticle.

$$G_r = \frac{W_{\text{g-LMW PLLA}}^{\text{g-SiO}_2}}{1 - W_{\text{g-LMW PLLA}}^{\text{g-SiO}_2}} \quad (1)$$

The TEM images of the SiO_2 and g-SiO_2 particles dispersed in PLLA–ESO matrix are shown in Fig. 4. As shown in Fig. 4a, it can be seen that the

number-average sizes of the SiO_2 nanoparticles are 40–50 nm which exhibit a strong tendency to aggregate. In order to overcome the problem of nonuniform dispersion, grafting of LMW PLLA onto the surface of SiO_2 nanoparticles shall be the subject of our consideration. Fortunately, after being surface grafted with LMW PLLA and dispersed by ultrasonic treatment, g-SiO_2 nanoparticles, as shown in Fig. 4b, can be easily dispersed into PLLA–ESO matrix to form a uniform PLLA–ESO/g-SiO_2 composite by solution mixing. This is because the LMW PLLA molecules are chemically linked onto the SiO_2 surface, good compatibility is expected between the SiO_2 nanoparticles and PLLA–ESO matrix.

Thermal properties of PLLA–ESO/g-SiO_2 and PLLA/g-SiO_2 composites

The thermal and crystallinity character of PLLA–ESO/g-SiO_2 nanocomposites with different g-SiO_2 contents were investigated by DSC (Fig. 5). The glass transition temperature (T_g), crystallization temperature (T_c), melting temperature (T_m), and melting enthalpy (ΔH_m) obtained from the DSC are summarized in Table 1. The crystallinity (χ_c) of PLLA–ESO/g-SiO_2 was determined from DSC measurements by the equation $\chi_c = \Delta H_m/\Delta H_m^0 \times 100/\chi$; with the aid of the enthalpy of fusion of 93.7 J/g for the perfectly crystalline PLLA [17], χ represents the percent of PLLA–ESO copolymer in PLLA–ESO/g-SiO_2 nanocomposites. As shown in Table 1, it was found that the crystallinity of the PLLA–ESO matrix increased with the increasing g-SiO_2 content from 2 to 8 wt% in the composites, which indicated that g-SiO_2 nanoparticles can serve as a nucleating agent for the crystallization of PLLA–ESO in the nanocomposites. However, the crystallinity of the PLLA–ESO matrix began to decrease gradually when the content was beyond 8%. It is mainly because too much silica in PLLA–ESO matrix hindered chain motion and ordered structure of the PLLA–ESO molecules. While the melting temperature (T_m) and the

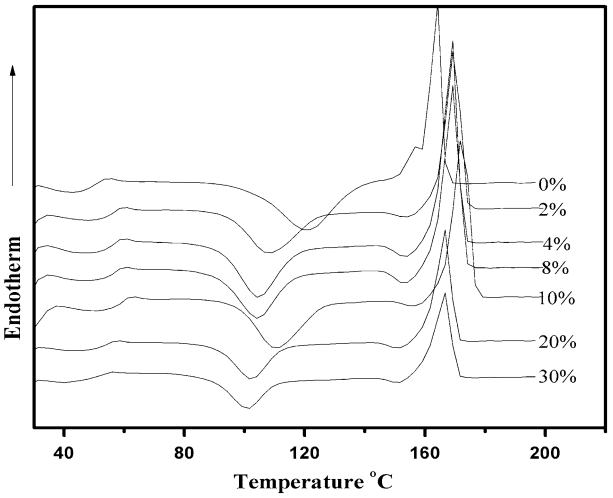

Fig. 5 DSC curves of PLLA–ESO/g-SiO_2 nanocomposites with various g-SiO_2 contents

Table 1 Thermal properties of PLLA–ESO/g-SiO_2 nanocomposites with different g-SiO_2 content determined by DSC

g-SiO_2 content (wt%)	T_g (°)	T_c (°)	T_m (°)	ΔH_m (J/g)	χ_c (%)
0	53.0	123.3	166.1	35.93	38.34
2	56.4	107.9	170.7	39.49	43.05
4	56.3	104.7	170.9	48.48	53.90
8	56.7	104.5	170.8	48.01	55.69
10	57.2	107.9	170.7	42.56	50.47
20	56.9	104.9	169.7	28.72	38.31
30	54.8	103.2	170.1	24.29	37.03

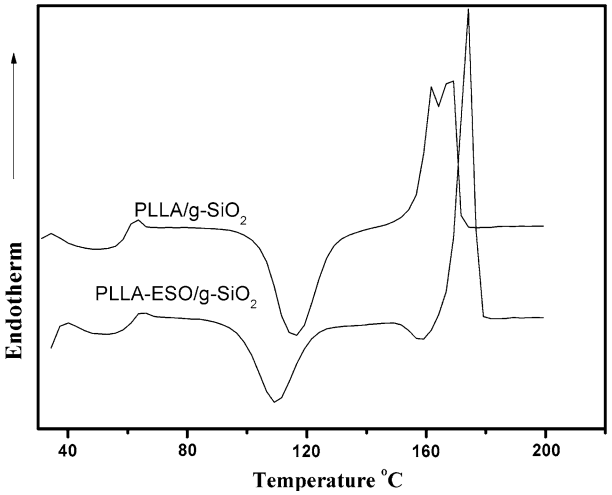

Fig. 6 DSC curves of PLLA–ESO/g-SiO_2 and PLLA/g-SiO_2 nanocomposites

glass transition temperature (T_g) seemed to be independent of loading of g-SiO_2 particles. Similar results can be found in other systems such as hydroxyapatite/PLLA nanocomposites [18].

In the second heating scan of DSC of PLLA/g-SiO_2 nanocomposite, double melting peaks appeared obviously, while PLLA–ESO/g-SiO_2 nanocomposites did not show this phenomenon (Fig. 6). This is due to slow crystallization rate of polylactic acid which led to its imperfect crystal of PLLA/g-SiO_2 nanocomposite. In the second heating scan, the less perfect crystals of PLLA/g-SiO_2 nanocomposite melted accompanied by absorption of heat at relatively low temperature, then re-crystallized and re-melted accompanied by endotherm, resulting in the double melting peaks. Due to the introduction of methylene soft segment of ESO, the flexibility of PLLA–ESO copolymer chain increases, furthermore, makes the PLLA–ESO/g-SiO_2 nanocomposite fully crystallized at 10 °C/min heating rate. Therefore, there is only a single melting peak.

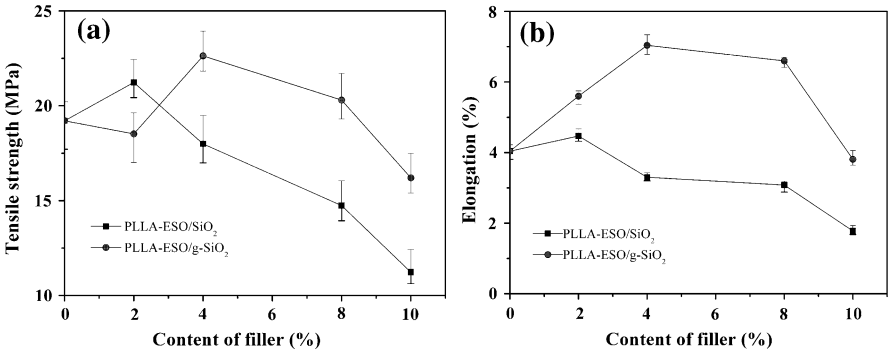

Fig. 7 Effect of the filler content on **a** tensile strength and **b** elongation at break of the PLLA–ESO/g-SiO_2 and PLLA–ESO/SiO_2 composites

Mechanical properties

The relationship between the tensile strength and the filler SiO_2 content of the composites is illustrated in Fig. 7a. In most cases, PLLA–ESO/g-SiO_2 composites had a higher tensile strength than that of PLLA–ESO/SiO_2 composites with the same filler content, except when the filler content is 2 wt%. This may be because that grafting of LMW PLLA onto the surface of SiO_2 nanoparticles enhanced the interface compatibility of PLLA–ESO matrix and SiO_2 nanoparticles, and thus, the PLLA–ESO/g-SiO_2 composites exhibit improved tensile strength.

Figure 7b showed the influence of particle loading on the elongation at break of the composites. In Fig. 7b, the elongation at break of PLLA–ESO/g-SiO_2 composites shows a maximum at 4 wt% g-SiO_2 loading. While the elongation of PLLA–ESO/SiO_2 composites decreases monotonously as SiO_2 content increases further. The improvement of elongation at break of PLLA–ESO/g-SiO_2 in compared to PLLA–ESO/SiO_2 composites is also ascribed to the presence of the g-SiO_2 nanoparticles. The LMW PLLA grafted onto the SiO_2 nanoparticles' surfaces forms a stable hindrance layer between particles which inhibit the agglomeration and thus improves the dispersibility of the SiO_2 nanoparticles in PLLA–ESO matrix greatly. Also, the interfacial combination between SiO_2 nanoparticles with PLLA–ESO matrix is enhanced greatly. Thus, the PLLA–ESO/g-SiO_2 composites exhibit improved elongation at break.

Conclusions

In the study, the surface of SiO_2 nanoparticles has been successfully modified by grafting LMW PLLA. FTIR and TGA analyses confirmed that the chemical reactions occur between the SiO_2 particles and the LMW PLLA. The grafting ratio of LMW PLLA was dependent on the reaction time, and the highest grafting ratio obtained was about 28.2%. The g-SiO_2 nanoparticles could be comparatively homogeneously dispersed in PLLA–ESO matrix, in contrast to the severe

aggregation of un-grafted SiO_2 nanoparticles. DSC analysis indicated that g-SiO_2 nanoparticles can serve as a nucleating agent for the crystallization of PLLA–ESO in the nanocomposites, while the T_m and the T_g of PLLA–ESO/g-SiO_2 nanocomposites seemed to be independent of loading of g-SiO_2 nanoparticles. Furthermore, PLLA/g-SiO_2 nanocomposite appeared double melting peaks, while PLLA–ESO/g-SiO_2 nanocomposites showed a single melting peak. In most cases, PLLA–ESO/g-SiO_2 composites had a higher tensile strength and elongation than that of PLLA–ESO/SiO_2 composites with the same filler content.

Acknowledgments The work was financially supported by The Key Technology R&D Program of Jiangsu (Project No. BE2010176), Natural science fund for colleges and universities in Jiangsu Province (Project No. 08KJB430004), Scientific and Technological Developing Scheme of Zhenjiang City (Project No. SH2008073).

References

1. Kale G, Auras R, Singh SP, Narayan R (2007) Biodegradability of polylactide bottles in real and simulated composting conditions. Polym Test 26:1049. doi:10.1016/j.polymertesting.2007.07.006
2. Garlotta D (2002) Literature review of poly(lactic acid). J Polym Environ 9:63. doi:10.1023/A:1020200822435
3. Li YJ, Shimizu H (2007) Toughening of polylactide by melt blending with a biodegradable poly(ether)urethane elastomer. Macromol Biosci 7:921. doi:10.1002/mabi.200700027
4. Signori F, Coltelli MB, Bronco S (2009) Thermal degradation of poly(lactic acid) (PLA) and poly(butylene adipate-co-terephthalate) (PBAT) and their blends upon melt processing. Polym Degrad Stab 94:74. doi:10.1016/j.polymdegradstab.2008.10.004
5. Anderson KS, Lim SH, Hillmyer MA (2003) Toughening of polylactide by melt blending with linear low-density polyethylene. J Appl Polym Sci 89:3757. doi:10.1002/app.12462
6. Lu JM, Qiu ZB, Yang WT (2007) Fully biodegradable blends of poly(L-lactide) and poly(ethylene succinate): miscibility, crystallization, and mechanical properties. Polymer 48:4196. doi:10.1016/j.polymer.2007.05.035
7. Zou J, Chen X, Shu Y, Zhou HJ, Huang FR (2010) Synthesis, characterization of star-shaped copolymers of L-lactide and epoxidized soybean oil. Polym Bull. doi:10.1007/s00289-010-0280-3
8. Tomalia DA, Dvornic PR (1994) What promise for dendrimers? Nature 372:617. doi:10.1038/372617a0
9. Fréchet JM (1994) Functional polymers and dendrimers: reactivity, molecular architecture, and interfacial energy. Science 263:1710. doi:10.1126/science.8134834
10. Trollsås M, Hedrick JL (1998) Dendrimers-like star polymers. J Am Chem Soc 120:4644. doi:10.1002/macp.200600614
11. Hyon SH, Jamshidi K, Ikada Y (1997) Synthesis of polylactides with different molecular weights. Biomaterials 18:1503. doi:10.1016/S0142-9612(97)00076-8
12. Sʹober W, Fink A, Bohn E (1968) Controlled growth of monodisperse silica spheres in the micron size range. J Colloid Interface Sci 26:62. doi:10.1016/0021-9797(68)90272-5
13. Rahman IA, Vejayakumaran P, Sipaut CS, Ismail J, Abu Bakar M, Adnan R, Chee CK (2007) An optimized sol-gel synthesis of stable primary equivalent silica particles. Colloids Surf A 294:102. doi:10.1016/j.colsurfa.2006.08.001
14. Li GS, Li LP, Smith JR, Inomata H (2001) Characterization of the dispersion process for $NiFe_2O_4$ nanocrystals in a silica matrix with infrared spectroscopy and electron paramagnetic resonance. J Mol Struct 560:87. doi:10.1016/S0022-2860(00)00772-9
15. Chen L, Qiu XY, Deng MX, Hong ZK, Luo R, Chen XS (2005) The starch grafted poly(L-lactide) and the physical properties of its blending composites. Polymer 46:5723. doi:10.1016/j.polymer.2005.05.053
16. Helwig E, Sandner B, Gopp U, Vogt F, Wartewig S, Henning S (2001) Ring opening polymerization of lactones in the presence of hydroxyapatite. Biomaterials 22:2695. doi:10.1016/S0142-9612(01)00015-1

17. Fischer EW, Sterzel HJ, Wegner G (1973) Investigation of the structure of solution grown crystals of lactide copolymers by means of chemical reactions. Polymer 251:980. doi:10.1007/BF01498927
18. Hong ZK, Zhang PB, He CL, Qiu XY, Liu AX, Chen L (2005) Nano-composite of poly(L-lactide) and surface grafted hydroxyapatite: mechanical properties and biocompatibility. Biomaterials 26:6296. doi:10.1016/j.biomaterials.2005.04.018